www.czasopisma.pan.pl PAN www.journals.pan.pl

Metrol. Meas. Syst., Vol. 29 (2022) No. 4, pp. 719–736
DOI: 10.24425/mms.2022.143072

METROLOGY AND MEASUREMENT SYSTEMS
Index 330930, ISSN 0860-8229
www.metrology.wat.edu.pl

EVALUATION OF NEW DESIGNED REFERENCE BLOCKS FOR CALIBRATION AND NDT BY OPTICAL AND ULTRASONIC TECHNIQUES

Mirham A.Y. Barakat[1], Mohamed Abdelwahab[2], Alshaimaa Waheed Abdallah[2]

1) *Ultrasonic Metrology Laboratory, National Institute of Standards PO Box: 136, Giza code 12211, Tersa Street, Haram, Giza, Egypt* (✉ *mirham75@yahoo.com*)
2) *Line & End Secondary Standards Laboratory, National Institute of Standards PO Box: 136, Giza code 12211, Tersa Street, Haram, Giza, Egypt* (*a.abdo73@yahoo.com*, +20 1065 695 164, *shimaawahid@yahoo.com*)

Abstract

Reference blocks are required for ultrasonic calibration and non-destructive testing (NDT). There are already in existence sets of reference blocks constructed according to American Society for Testing and Materials standards, but as the industry evolves, we need more reference blocks with varied designs. In this study, two reference blocks of steel and aluminum are constructed. These blocks have several sets of flat bottom holes (FBH) with different diameters (0.5, 1, 1.5, 2 and 2.5 mm), angles (45° and 90°) and placements. The novel constructed reference blocks are evaluated using the ultrasonic and a displacement measuring interferometer (DMI). They allow for detailed FBH characterization in terms of defining their location, diameter, depth and so on. The two techniques show consistency in the majority of the outcomes. The expanded uncertainty of readings is found to be ±1.4 µm, according to DMI data. The findings show that the newly constructed blocks could be ideal for evaluating a variety of calibration factors including transducer sensitivity, dead zone, defect size, and depth. Furthermore, they can be used in NDT in various industries such as petroleum pipe production, steel manufacturing and so on.

Keywords: calibration, reference blocks, ultrasonic, displacement measuring interferometer (DMI).

1. Introduction

Ultrasonic testing (UT) is one of the *non-destructive tests* (NDT). It allows the determination of surface, subsurface, internal and dimensional defects, and therefore, it can perform a thorough volumetric investigation of materials. The frequency range for ultrasonic NDT is usually between 1 and 30 MHz [1].

There are two main ultrasonic operational modes: pulse echo and through transmission. The choice of mode depends on the test purpose. In many tests, the pulse-echo method is preferred because it can examine a wide range of defects, including their size, area and location inside the material. It also includes a single coupling region between the transducer and the specimen

Article history: received June 3, 2023; revised September 5, 2022; accepted September 12, 2022; available online October 13, 2022.

(for both transmission and reception of waves). As a result, it is a simple approach with constant conditions [2].

To perform UT, calibration must be first performed. Calibration ensures the validation of the test, *i.e.* it standardizes the equipment to correctly do the test. For example, if we need to calibrate an ultrasonic thickness gauge, standard blocks of well-defined dimensions are needed. Then we calculate the deviation errors of the obtained measurements from the standard values. Also, to calibrate a reference block, its dimensions and defects are determined using an ultrasonic echo meter or ultrasonic flaw detector, then a comparison of measurements is done. The comparison is made between the measured values of the tested block and the data in the calibration certificate of this block or the data from another standard primary block that has the same shape and dimensions as the tested block. Many calibration procedures can be followed according to standards like ASTM, DIN, *etc.*

Generally, calibration in UT is used in a variety of industries, including nuclear, steel, gas and oil and so on. Reference or calibrated blocks are used in UT by the user to validate the desired operation. Specific calibration demands, such as thickness calibration, transducer sensitivity calibration, beam profile analysis calibration and on the like, are met by reference blocks. Aluminum, steel, stainless steel and titanium are used to create the reference blocks. They come in a variety of shapes, including grooves, holes, curved surfaces and other features. Reference standards are representative tools designed to meet ASTM, ASME, AMS, ISO and many other specifications. They are used to standardize responses from testing equipment. Samples with defects like notches and *Flat-bottom Holes* (FBH) are often used to standardize the amplitude of the detected signal concerning the size and/or position of known reflectors. *Side-drilled holes* (SDH) are also an effective target for such standardizations.

Many reference blocks have been manufactured in accordance with ASTM E127 and ASTM E428 [3, 4]. The 30 FBH resolution reference block, for example, has crucial calibration features such as transducer sensitivity, transducer resolution, flaw size and flaw depth. To determine the transducer dead zone, sensitivity and distance-area amplitude, ASTM distance/area–amplitude blocks (a set of 10) are used. The ASTM distance-amplitude #3, #5 and #8 FBH blocks (a set of 19) can be used to determine the relationship between metal distance and signal amplitude. In general, the American Society for Testing and Materials (ASTM) had presented many blocks designed to meet various calibration and test requirements. In 1958, they published the first official standard document on flat-bottomed-hole reference blocks manufactured of aluminum alloy as a defect artifact standard in ultrasonic nondestructive testing. Apart from this, there are several firms producing blocks in accordance with industry needs. *Flat bottom holes* (FBH) were used to demonstrate transducer sensitivity and characterize distinct holes on these constructed blocks. These blocks were typically rectangular in shape, with single-sized FBH positioned at various locations on the block surface [5].

FBH calibration blocks can be evaluated using optical techniques. Non-contact and contact methods can be used to measure the dimensional measurements of the planned holes, such as position, diameter, and depth. Contact techniques such as cylinder gauges, micro indicators, calipers and other similar instruments have lower resolution and accuracy than non-contact approaches [6–8]. Measuring the interior diameter is challenging because contact techniques detect the exterior diameter of holes by making contact with the surface. When applied to measure the dimensions and inner diameter of holes, optical non-contact techniques such as laser interferometry, profile projection, electro-optical method and optical machines are highly precise [9, 10]. In length and dimensional metrology measurements, the secondary standard is a stabilized wavelength laser. The *displacement measuring interferometer* (DMI) is made up of a heterodyne stabilized wavelength laser and optical components, as well as a motorized moving

Metrol. Meas. Syst., Vol. 29 (2022), No. 4, pp. 719–736
DOI: 10.24425/mms.2022.143072

stage and a magnifying microscope [11]. Because it relies on a stable wavelength laser to measure and calibrate the position, inner diameter and depth of the planned holes on steel and aluminum reference blocks, DMI is the most accurate, precise and high-resolution technique. The detection of the displacement between the positions of each interior wall of the measuring holes is required for inner diameter measurements. The displacement between the positions of the surface and the bottom of the holes is used to determine the depth. The optical constants of the Steel and Aluminum reference blocks were determined using a PHE-103Ellipsometer [12].

As previously stated, most built calibration blocks had a single-sized FBH at the right angle and positioned at various locations on the block surface. The aim is to improve the data used to assess transducer sensitivity. Varying FBHs of different angles (45° and 90°) and different sizes are designed into rectangular aluminum and steel blocks. As a result, measurement variability increased and also the accuracy of detection sensitivity. In addition, these new blocks will be used to test the performance of the ultrasonic examination apparatus and search units as well as to standardize and control ultrasonic testing of metal alloy items. In this study, the newly developed blocks are calibrated, evaluated and assessed using ultrasonic and DMI techniques.

2. Experimental details

The newly designed reference blocks are evaluated using both calibration and non-destructive tests. Therefore, we drilled many holes with different shapes by varying their diameters, angles and positions which offers multiple tests in just two reference blocks that were made from steel and aluminum. Steel and aluminum materials are the most commonly used materials to design reference blocks according to ASTM standards. These reference blocks offered newly designed holes that are not made in any other standard blocks as it poses quite a challenge to serve the calibration better as well as the needs of the non-destructive tests that are in continuous progress due to industry development.

Reference standards must be prepared and used in accordance with well-designed specifications that cover the material selection, the manufacture of artificial defects and of course, instructions for the specific testing application.

2.1. Blocks material

According to ASTM [13], the reference steel block was made of steel 4340 and the reference aluminum alloy block was constructed of aluminum alloy 7075-T6 according to ASTM [14]. METLINE, India, provided the materials.

2.2. Block design

Steel (St4340) cuboid shape block with five sets of FBH of varying sizes (Q = 0.5, 1, 1.5, 2 and 2.5 mm) and similar drilling depth (D = 5 mm), each set consisting of four FBH of the same diameter but varied position with regard to the block surface, *i.e.*, the steel block had 20 FBH. Cuboid aluminum alloy (Al7075-T6) block designed to have four sets of FBH of different diameters (1, 1.5, 2 and 2.5 mm) and the same depth, each set composed of two FBH of the same diameter but different position with respect to the block surface, *i.e.*, the aluminum alloy block had eight FBH, as shown in Figs. 1 and 2. The steel block dimensions were $2 \times 3 \times 22$ cm^3 and its FBH was at a straight angle. The dimensions of the aluminum alloy block were $2 \times 3.5 \times 23$ cm^3 and it had an inclined FBH at 45°. The FBH was drilled with drilling mechanical equipment (a Radial Drilling Machine by IndiaMart.com). The drilling depth inside the steel block was 5 mm, however, it ranged from 6 to 14 mm for aluminum blocks.

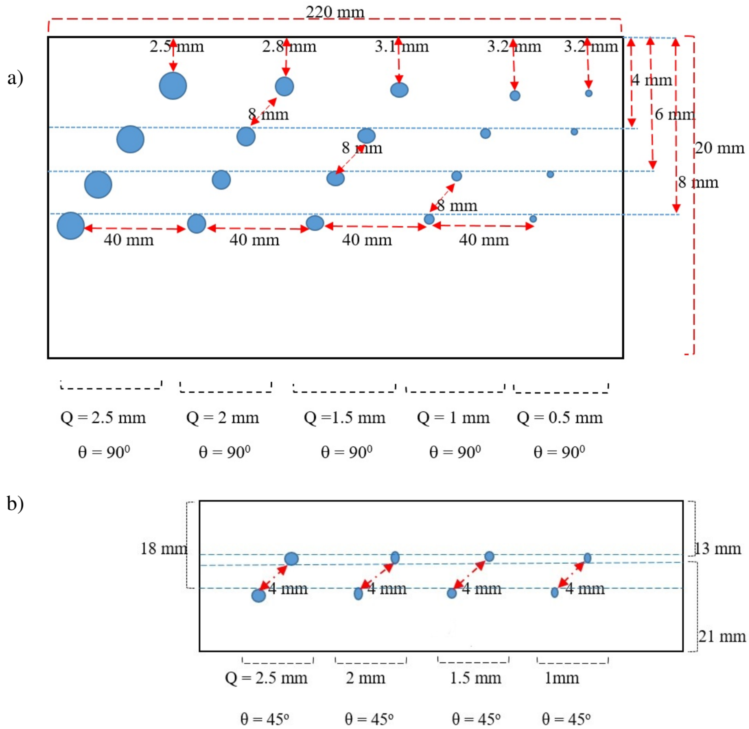

Fig. 1. Design of a) steel block front and b) aluminum block front (Note that Q is FBH diameter, θ is FBH angle and the surfaces of blocks are smooth).

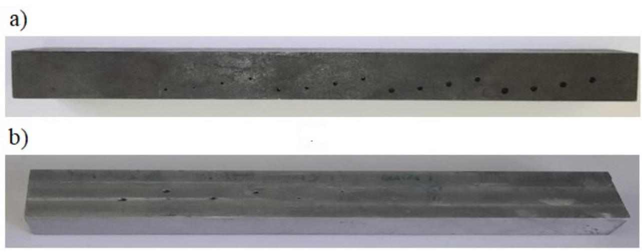

Fig. 2. Photos of (a) the steel block and (b) the aluminum alloy block.

The new reference blocks were manufactured using a drilling machine with different driller tips to attain different hole diameters. The block was first machined with the desired dimensions, then we drew points on the block to mark the position of the holes. To obtain the angled holes the block was adjusted on an angled wedge then the holes were drilled. A water supply was used to cool the driller tip. After completing the drilling process, the water was evaporated using hot air.

The newly designed steel block was coded MIR01ST, while the newly designed aluminum block was coded MIR02AL. The type and density of both blocks are represented in Table 1.

Metrol. Meas. Syst., Vol. 29 (2022), No. 4, pp. 719–736
DOI: 10.24425/mms.2022.143072

Table 1. Type and density of the newly designed blocks.

New blocks	Type	Density, Kg/m^3
MIR01ST	St4340	7850
MIR02AL	Al7075-T6	2800

2.3. Ultrasonic measurement facility

The employed ultrasonic measuring equipment was evaluated to check its measurement performance according to BS EN 12668-3:2000 [15]. Only pulse-echo equipment A-scan presentations comprising direct contact testing are covered by the approaches.

2.3.1. Transducer

Ultrasonic transducers have been calibrated according to BS EN 12668-2:2001 [16]. Their nominal frequencies are 2 and 4 MHz. In order to record their beam profiles, we used an ultrasonic flaw detector (USIP 20 by Krautkramer Branson), a vector signal analyzer (IF (89441A by HP) and an oscilloscope (TDS 3052B by Tektronix (USA)). The transducer parameters are listed in Table 2.

Table 2. Transducer parameters.

Transducer	Damping factor	Peak frequency (f_0), MHz	Upper frequency (f_u), MHz	Lower frequency (f_l), MHz	Bandwidth (BW), MHz
S12HB2	1/4	2.1	3.6	0.9	2.7
S12HB4	1/3	4	5.3	1.6	3.7

The measurement results were traceable to the SI units, the temperature was 21.4°C ±1°C and the humidity was 58.6% ± 5%.

2.3.2. Ultrasonic test instrument

The ultrasonic equipment is composed of a normal transducer (S12HB2 by Karl Deutsch), shear transducer of 2 MHz (S12Y2 by Karl Deutsch), flaw detector (USN 60 by GE Inspection Technologies), oscilloscope (WaveJet 354A by Lecroy,) and reference blocks (VI, VII and a Navship cylindrical reflector block, 1018 steel, S. N. A14786).

2.3.3. Equipment standardization

The flaw detector was calibrated according to ASTM E 317-16. The expanded uncertainty using a coverage factor of 2, providing a level of confidence of approximately (95%) is U_{exp} = ±0.003, the temperature was 22.1°C ±1°C and the humidity was 25% ± 5%.

Linearity of amplification: The divergence from linearity was plotted against the echo number in Table 3. The flaw detector was set to 10 echoes on the flaw detector screen, after which each echo was gated and the gain was boosted by 6 dB and the echo height was recorded. For each echo, these processes were repeated three times. The average deviation was then determined. The amplifier was determined to be linear with a 0.05 average deviation.

Table 3. Linearity of amplification.

Echo No.	Deviation from linearity
1	0.03
2	0.01
3	0.01
4	0.02
5	0.01
6	0.02
7	0.03
8	0.01
9	0.02
10	0.03

Time base linearity and resolution: The time base of the instrument was linear within throughout range. The probe delay is 0.57 µs. The equipment was capable of distinguishing the different surfaces of the ultrasonic standard reference block.

Penetration power: Five echoes were obtained from the cylindrical Perspex piece of the ultrasonic standard reference block VI, at maximum gain with a low echo to noise ratio, with an accepted signal to noise ratio indicating a good penetrating power.

2.3.4. Standard reference block

Standard reference block (Navship cylindrical reflector block, 1018 steel, S. N. A14786) was calibrated according to ASTM E797/E797M-15 [17] and E317-16 [18] after flaw detector and transducer calibration. This calibration was performed using the same equipment that was used to test the newly designed blocks in order to determine the standard deviations of the data and to ensure that the equipment system was appropriately calibrated to ensure proper calibration of the new blocks. The extended uncertainty using the coverage factor of 2, with a level of confidence of about 95% was $U_{\text{exp}} = \pm 0.01$ mm, with a temperature of 19.6°C ±1°C and a humidity of 62% ± 5%. It is worth noting that the standard reference block contained six 1 mm diameter FBHs in various locations on its surface.

2.4. Optical test method

Because DMI is applied as a secondary standard for length and dimensions measurements, the optical measurements produced by DMI are used to verify the measurements obtained with the ultrasonic method. The diameter and depth of a number of planned holes in steel and aluminum blocks are measured using a high-resolution digital heterodyne displacement interferometer. Figure 3a shows the measuring system of the inner diameter of the roundness of the holes and Fig. 3b shows the measured system for measuring their depth. A Zygo laser head, polarizing beam splitter, retroreflector mirrors, fiber cable with pick up and measuring board with software make up the displacement interferometer. A computerized travelling stage and a magnifying microscope are also available for inspecting the delicate edge of the holes.

The Zygo laser head emits a beam consisting of two orthogonal linear polarizing beams of frequencies f_1 and f_2 which are separated by nearly 20 MHz. Frequencies f_1 and f_2 are related

Metrol. Meas. Syst., Vol. 29 (2022), No. 4, pp. 719–736
DOI: 10.24425/mms.2022.143072

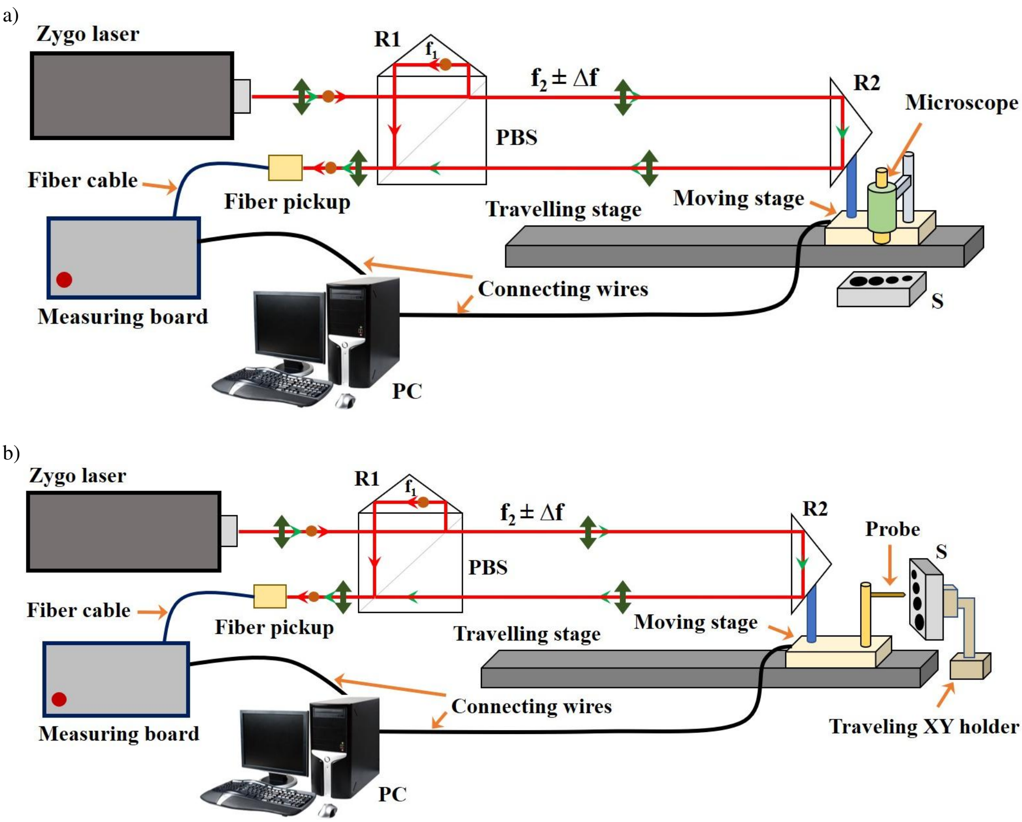

Fig. 3. Displacement measuring interferometer DMI setup a) for diameter measurements, b) for depth measurement; R1, R2: reference and measured retroreflectors, PBS: polarizing beam splitter, S: sample.

to wavelengths 632.991501 nm and 632.991528 nm respectively. The two beams travel toward a polarizing beam splitter that is used to separate the two orthogonal polarizing beams f_1 and f_2. The reference beam of frequency f_1 is directed toward the fixed retroreflector and the other beam of frequency f_2 is directed toward a moving retroreflector. The two reflected reference and measured beams are recombined and emerge from the polarizing beam splitter to produce an optical interference signal. This interference signal is transferred through a fiber cable to the measuring board for converting it into digital data.

In displacement measurement, beam f_1 becomes the reference beam since it moves a fixed distance path. Beam f_2 is the measured beam since it travels toward the target retroreflector which moves a distance to yield a beam of frequency $f_2 \pm \Delta f$ that is reflected back to the interferometer. The motion of the target retroreflector causes a Doppler shift in the reflected beam. The measuring board receiver detects a signal, which is the frequency difference between the reference and measured beams and given by $f_1 f_2 \pm \Delta f$. This signal is compared with the reference signal $f_1 f_2$ on the measuring board.

The desired displacement d is calculated through the equation [19]:

$$d = \frac{1}{N}\frac{\varphi}{M}\frac{\lambda_{\text{vac}}}{n}, \tag{1}$$

where φ is the phase, λ_{vac} is the vacuum wavelength, n is the refractive index of the medium, N is an integer based on a number of passes and M is a constant depending on the measurement electronics. M value refers to the number of phase meter counts per 2π radians of the phase. The wavelengths collected from the laser head are slightly different in frequency and based on that the measurement arm calculates the suitable wavelength value. Using the erroneous wavelength results in displacement inaccuracy. Because a change in the refractive index causes a change in the wavelength, the refractive index must be precisely set for operation in a medium other than vacuum.

According to the Edlén equation [20], a computerized high-resolution digital sensor is used to record environmental factors such as air temperature, pressure and humidity in order to correct the wavelength of light due to the influence of the refractive index of air.

The target mirror and magnifying microscope were mounted on a travelling linear motorized stage (Model IMS600LM by Newport) with a minimum incremental motion of 20 nm and repeatability of 0.05 µm for the diameter measurements of the holes shown in Fig. 3a. The magnifying microscope was utilized to precisely determine the tiny edge of the hole. The change in location of the target mirror from the zero position or beginning point is measured during the measurements. The interferometer must mark it as zero at one edge of the hole and then move it to the other edge where the values of the moved distance are recorded using the magnifying microscope. For establishing the maximum diameter of roundness, the measured diameter is repeated a number of times over the curvature of the holes.

As shown in Fig. 3, the depth of the hole was determined by replacing the magnifying microscope with a very small probe (b). To begin, we placed the probe against the hole outer surface and re-zerod the interferometer, which served as a measuring start point. After zeroing the probe, it moved within the hole until it came into touch with its bottom, when the depth was recorded. The whole measurement sequence was performed a number of times at different sites for a correct depth determination.

The optical constants of steel and aluminum blocks were determined with the PHE-103 ellipsometer at wavelengths ranging from 250 nm to 1000 nm with a fixed incidence angle of 70° [21]. It was achieved by measuring the ellipsometric parameters Δ, Ψ, which indicated the phase and amplitude shift in the light beam after it had been reflected from the surface of the test item [22]. These factors were needed to calculate the object's optical constants, such as the refractive index n and extinction coefficient k [23].

3. Results and discussion

3.1. Block properties

3.1.1. Ultrasonic velocity (C), Poisson's ratio (ν), elastic moduli (E, L, G and K) and micro-hardness (H)

The ultrasonic operation mode is the direct contact ultrasonic operation utilizing the pulse echo technology. In this operation, the ultrasonic transducer acted as transmitter and receiver of echoes at the same time and it had one coupling point on the block's surface. The ultrasonic velocity (C) and the mechanical parameters were determined. The ultrasonic velocity (C) was determined by means of block's thickness (x) and the time travelled by the echoes (t) as follows:

$$C = \frac{2x}{t} . \tag{2}$$

Metrol. Meas. Syst., Vol. 29 (2022), No. 4, pp. 719–736
DOI: 10.24425/mms.2022.143072

By the use of the measured ultrasonic longitudinal (C_L) and shear (C_S) velocities, some blocks properties including the Poisson's ratio (v), elastic moduli (E, L, G and B) and micro-hardness (H) were calculated as follows [24]:

$$v = \frac{1 - 2\left(C_S/C_L\right)^2}{2 - 2\left(C_S/C_L\right)^2}, \tag{3}$$

$$\rho E = 2(C_S)^2(1 + v), \tag{4}$$

$$\rho L = (C_L)^2, \tag{5}$$

$$\rho G = (C_S)^2, \tag{6}$$

$$B = L - \left[\left(\frac{4}{3}\right) G\right], \tag{7}$$

$$H = \left[\frac{(1 - 2v)E}{6(1 + v)}\right], \tag{8}$$

where C_L is ultrasonic longitudinal velocity, C_S is ultrasonic shear velocity, v is the Poisson's ratio, ρ is block density, E is Young's modulus, L is the longitudinal modulus, G is the shear modulus, B is the bulk modulus and H is the micro-hardness.

Table 4 shows that a steel block (MIR0ST) had higher elastic properties (Young's (E), longitudinal (L), shear (G) and bulk (B) moduli) than the aluminum block (MIR02AL), as well as higher micro-hardness (H). The ultrasonic longitudinal velocity of the steel block is smaller than that of the aluminum block but the shear velocity did the contrast. These last-mentioned features were used to evaluate and record the most essential aspects of the blocks. MIR01ST is harder, with fewer interatomic gaps, than MIR02AL.

Table 4. Some calculated block properties.

Blocks	**C_L (m/s), ± 40 m/s**	**C_S (m/s), ± 40 m/s**	**v**	**E (GPa)**	**L (GPa)**	**G (GPa)**	**B (GPa)**	**H (GPa)**
MIR01ST	5890	3234	0.284	210.9	272.3	82.1	162.9	11.8
MIR02AL	6320	3113	0.34	73	112.2	27.2	75.9	2.9

3.1.2. Optical constants of the newly designed blocks

Selected optical properties of the blocks, *i.e.*, the optical constants the refractive index (n) and the extinction coefficient (k) of both aluminum and steel blocks which were determined using the PHE-103 ellipsometer at an angle of incidence 70° and in the wavelength range from 250 nm to 1000 nm [25, 26] are shown in Fig. 4a and 4b.

From Fig. 4 it can be seen that both the refractive index and the extinction coefficient increased with wavelength in both blocks. In the aluminum block, the refractive index ranged from about 0.3 to about 2.3 and the extinction coefficient ranged from about 1.5 to about 7.3. In the steel block, the refractive index ranged from about 0.8 to about 2.5 and the extinction coefficient ranged from about 0.8 to about 2.8. The optical constants (refractive index & extinction coefficient) results of both the steel and aluminum materials show a good match with the data in the literature [31].

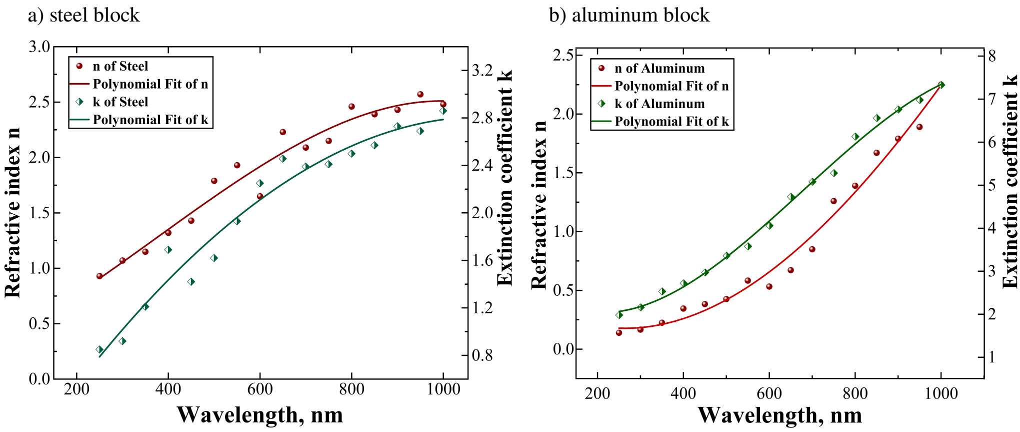

Fig. 4. The optical constants n and k measurements determined with the PHE-103 ellipsometer at different wavelengths range from 250 nm–1000 nm of a) steel block, b) aluminum block.

3.2. Block assessment

To make block assessment, a calibration procedure was performed according to ASTM E 428-92 [13] and ASTM E 127-92a [26]. The calibration procedure was as follows:

- Blocks cleaned of oil, dust, etc., using 70% ethanol.
- All measurements performed with pulse-echo ultrasonic testing using the equipment described in the experimental part.
- Ultrasonic velocity measured according to ASTM E 494-92a [27].
- Location of FBH from the block surfaces determined using the ultrasonic.
- Diameter and depth of FBH in the two newly designed blocks determined using ultrasonic and DMI technique. Note that DMI was used for verification and calibration of the dimensional measurements done with the ultrasonic technique.
- DMI technique used according to Length Scale Measurement Procedures [28].

3.2.1. Location of FBH from the blocks' surfaces

Figures 1a and 1b show the FBHs drilled at specific locations from the surface of the steel block (MIR01ST) and the aluminum block (MIR02A0L) and these locations are represented as nominal location (X) in Table 5. To verify these sites, the ultrasonic pulse echo method and the displacement measuring interferometer DMI were applied, as presented in Table 5. To calculate the measurement error, each position was measured ten times.

According to the data in Table 5, the values of average locations measured with the ultrasonic and DMI were virtually identical to those of nominal locations. The smallest deviation error for ultrasonic measurements was 0.02 mm and the largest was – 0.95 mm while the smallest deviation error for DMI measurements was – 0.0096 mm and the largest was 1.9656 mm.

The *standard error of the mean* (SEM) values are calculated in accordance with the position of the holes and the diameter for both ultrasonic and DMI techniques and are represented in Fig. 5a, b. In the figure, the SEM is plotted against the diameter of the holes. Each curve in the figure represents the hole position according to the location as referred to in the second column in Table 5. As shown in Fig. 5, all the standard errors of the mean values are random values.

Metrol. Meas. Syst., Vol. 29 (2022), No. 4, pp. 719–736
DOI: 10.24425/mms.2022.143072

Table 5. Location of FBHs in MIR01ST and MIR02AL.

Groups of FBHs	Hole positions	Nominal location (X), mm	Average location by the ultrasonic (X^{-}), mm	Deviation error ($X - X^{-}$), mm from the ultrasonic	Average location by DMI (X^{-}), mm	Deviation error ($X - X^{-}$), mm from DMI
MIR01ST: FBH 0.5 mm diameter	1	3.2	2.94	0.26	3.7099	–0.5099
	2	4	3.58	0.42	4.6110	–0.611
	3	6	5.92	0.08	6.6485	–0.6485
	4	8	8.06	–0.06	8.5427	–0.5427
MIR01ST: FBH 1 mm diameter	1	3.2	3.02	0.18	3.4208	–0.2208
	2	4	3.89	0.11	4.3888	–0.3888
	3	6	5.98	0.02	6.4337	–0.4337
	4	8	8.20	–0.20	8.3646	–0.3646
MIR01ST: FBH 1.5 mm diameter	1	3.1	3.15	–0.05	3.1125	–0.0125
	2	4	4.18	–0.18	4.1069	–0.1069
	3	6	6.03	–0.03	6.1504	–0.1504
	4	8	8.36	–0.36	8.1341	–0.1341
MIR01ST: FBH 2 mm diameter	1	2.8	2.38	0.42	2.7667	0.0333
	2	4	4.31	–0.31	3.6751	0.3249
	3	6	6.13	–0.13	5.8095	0.1905
	4	8	8.56	–0.56	7.8650	0.135
MIR01ST: FBH 2.5 mm diameter	1	2.5	2.57	–0.07	2.5096	–0.0096
	2	4	4.50	–0.50	3.6103	0.3897
	3	6	6.42	–0.42	5.6513	0.3487
	4	8	8.95	–0.95	7.6237	0.3763
MIR02AL: FBH 1 mm diameter	1	13	13.04	–0.04	14.212	1.212
	2	18	18.01	–0.01	19.9656	1.9656
MIR02AL: FBH 1.5 mm diameter	1	13	13.08	–0.08	14.074	1.074
	2	18	18.03	–0.03	19.7071	1.7071
MIR02AL: FBH 2 mm diameter	1	13	13.14	–0.14	13.564	0.564
	2	18	18.20	–0.20	17.9067	–0.0933
MIR02AL: FBH 2.5 mm diameter	1	13	13.26	–0.26	12.3237	–0.6763
	2	18	18.36	–0.36	18.3836	0.3836

When comparing the results of FBH location determination in the designed new blocks to those of FBH location determination in the standard reference block (Navship cylindrical reflector block, 1018 steel, S. N. A14786), we found that we obtain the same expanded uncertainty (U_{exp} = ±0.01 mm as for the standard reference block using the same equipment set and procedure (Navship cylindrical reflector block, 1018 steel, S. N. A14786). As a result, the newly constructed blocks can be used to correctly evaluate near-surface resolution in the same way that standard reference blocks do (Navship cylindrical reflector block, 1018 steel, S. N. A14786).

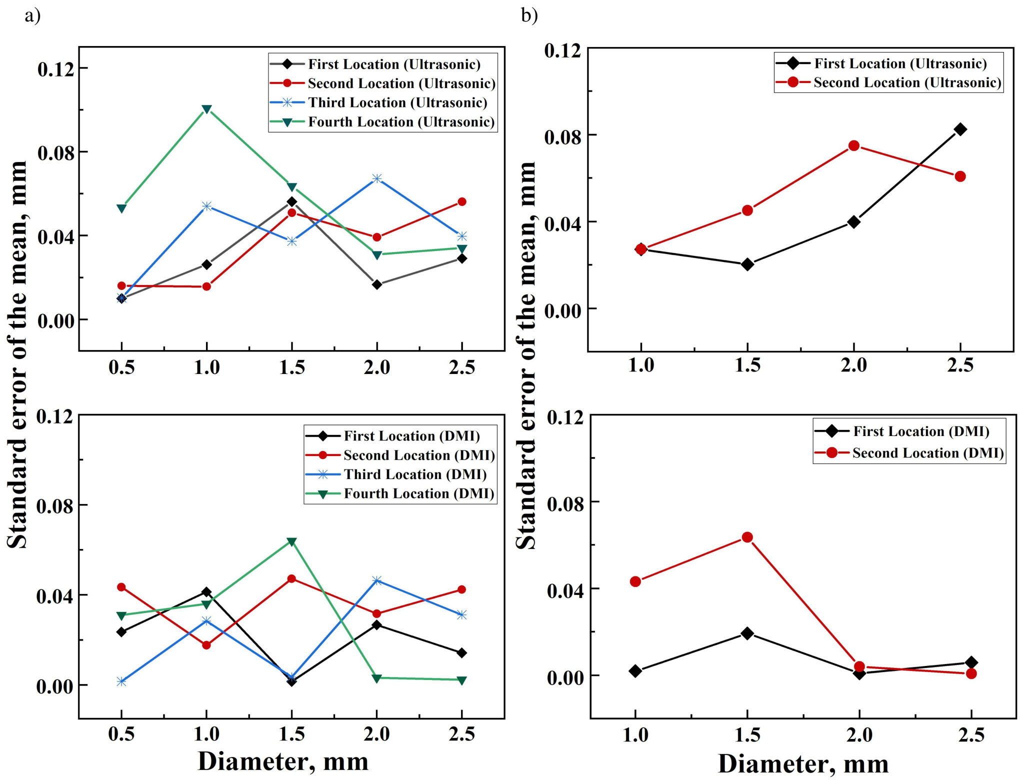

Fig. 5. Relation between the standard error of the mean SEM and the location of the holes
a) steel block and b) aluminum block.

3.2.2. Diameter and depth of FBH in the two new designed blocks

The FBH drilled diameters in the steel block (MIR01ST) shown in Fig. 1a, *i.e.* ranging from 0.5 mm to 2.5 mm, are represented as Groups 1 to 5 in Table 6, while the FBH drilled diameters in the aluminum block (MIR02AL) shown in Fig. 1b, *i.e.* ranging from 1 mm to 2.5 mm are represented in Groups 6 to 9 in Table 7. To verify these dimensions, the ultrasonic pulse echo and DMI techniques were applied. Each dimension was measured ten times with each technique in order to quantify the measurement error, as well as the depth of FBH drilling in the blocks, which was measured ten times and the error was calculated. Table 6 shows the diameter and depth measurements taken with the DMI and ultrasonic techniques on several sets of holes on a steel block (MIR01ST). The diameter and depth measurements of multiple sets of holes on an aluminum block (MIR02AL) using both methods are shown in Table 7.

The results in Tables 6 and 7 show a good agreement between the ultrasonic and DMI techniques. Table 6 shows that the DMI methodology was unable to measure the depth for the Group 5 MIR01ST, FBH 0.5 mm diameter, while Table 7 shows that both methods were unable to record the depth for the Group 9: MIR02AL, FBH 1 mm diameter.

When comparing the results of FBH diameter and depth determination in the designed new blocks to those of FBH location determination in the standard reference block (Navship cylindrical reflector block, 1018 steel, S. N. A14786), we found that we obtain the same expanded

Metrol. Meas. Syst., Vol. 29 (2022), No. 4, pp. 719–736
DOI: 10.24425/mms.2022.143072

Table 6. Results of diameter and depth measurements of holes on steel block (MIR01ST) using the DMI and Ultrasonic techniques.

Groups of FBHs	**Diameter by DMI (mm)**	**Diameter by Ultrasonic (mm)**	**Depth by DMI (mm)**	**Depth by Ultrasonic (mm)**
Group 1: MIR01ST, FBH 2.5 mm diameter				
1	2.5756	2.5501	6.3164	5.9124
2	2.6358	2.5903	6.1195	5.7402
3	2.7747	2.6320	6.0467	5.8706
4	2.7565	2.6197	6.1329	5.9102
Group 2: MIR01ST, FBH 2 mm diameter				
1	2.0615	2.0263	5.4647	5.2014
2	2.1146	2.0945	5.6395	5.6175
3	2.1252	2.1013	5.6528	5.4260
4	2.1384	2.1205	5.6998	5.5738
Group 3: MIR01ST, FBH 1.5 mm diameter				
1	1.5327	1.5215	5.7082	5.4860
2	1.5524	1.5411	5.6763	5.5324
3	1.5317	1.5302	5.6137	5.7105
4	1.5706	1.5614	5.5291	5.6081
Group 4: MIR01ST, FBH 1 mm diameter				
1	1.0253	1.0145	5.6325	5.5750
2	1.0395	1.0335	5.6582	5.7106
3	1.04127	1.0356	5.5114	5.6280
4	1.0516	1.0490	5.6522	5.5874
Group 5: MIR01ST, FBH 0.5 mm diameter				
1	0.5362	0.5129	NA	5.3808
2	0.5494	0.5358	NA	5.1962
3	0.5512	0.5471	NA	5.3460
4	0.5745	0.5602	NA	5.2765

Table 7. Results of diameter and depth measurements of holes on the aluminum block using the DMI and Ultrasonic techniques.

Groups of FBHs	**Diameter by DMI (mm)**	**Diameter by Ultrasonic (mm)**	**Depth by DMI (mm)**	**Depth by Ultrasonic (mm)**
1st Group 6: MIR02AL, FBH 2.5 mm diameter				
1	2.6372	2.6405	13.2157	13.7125
2	2.7766	2.7035	5.9895	6.1235
2nd Group 7: MIR02AL, FBH 2 mm diameter				
1	2.0175	2.0477	13.1643	13.4822
2	1.9685	2.0332	10.1135	10.3214
3rd Group 8: MIR02AL, FBH 1.5 mm diameter				
1	1.3994	1.5120	7.8969	8.0523
2	1.4543	1.5171	7.1094	7.4120
4th Group 9: MIR02AL, FBH 1 mm diameter				
1	0.9186	1.1240	NA	NA
2	0.8948	1.0447	NA	NA

uncertainty (U_{exp} = ±0.02 mm. As a result, the novel designed blocks are like standard reference blocks (Navship cylindrical reflector block, 1018 steel, S. N. A14786), *i.e.*, they can used to accurately test both defect diameter and depth, in addition, to calibrate ultrasonic equipment such flaw detectors, transducers, etc.

3.2.3. Angle of FBH in aluminum block (MIR02AL)

The angled FBH in the aluminum block (MIR02AL) was measured using an angle probe (MWB 45°, 4 MHz, 56927-19452 by Krautkramer). The angle adjustment was set to 45°. The average angle measurement (A) was calculated after 10 repetitions.

As shown in Table 8, the deviation varied from –0.4° to 0.3°. Therefore, the designed aluminum block can served as a good reference block to estimate the inclined angle of a given reflector.

Table 8. Angle of FBH in the aluminum block (MIR02AL).

Groups of FBHs	**Angle measured by ultrasonic (A^-), (°)**	**Deviation from a nominal angle (45°–A^-), (°)**
Group 6: MIR02AL, FBH 2.5 mm diameter		
1	44.7°	0.3°
2	45.4°	–0.4°
Group 7: MIR02AL, FBH 2 mm diameter		
1	45.2°	–0.2°
2	45.3°	–0.3°
Group 8: MIR02AL, FBH 1.5 mm diameter		
1	44.9°	0.1°
2	44.9°	0.1°
Group 9: MIR02AL, FBH 1 mm diameter		
1	45°	0°
2	45.1°	–0.1°

3.3. Uncertainty of diameter and depth measurements using DMI

The uncertainty in measuring the hole diameter and depth estimated according to the ISO guide to the Expression of Uncertainty in Measurement [29] is shown in Table 9. The main sources of uncertainty are the wavelength of the laser, the air refractive index due to the change in the environmental conditions (temperature, humidity and pressure), thermal expansion of the materials, the cosine error and finally the repeatability of the measurements.

The model equation which includes all the parameters that contribute to the diameter and depth measurement process is expressed as:

$$l = l_{\text{laser}} + l_t + l_\alpha + l_{\text{res stage}} + l_{\text{res software}} + l_{\cos} + l_{\text{refractive index}(t,p,RH)} + l_{\text{geometry}} + l_{\text{interferometer}} + l_{\text{repeatability}} . \tag{9}$$

The certified uncertainty in the laser wavelength is ±2 nm which contributed to uncertainty (diameter, depth) by ±0.001 µm. The temperature of the blocks must be recorded during the measurement process to calculate the deviation that occurred in temperature. The contribution

Metrol. Meas. Syst., Vol. 29 (2022), No. 4, pp. 719–736
DOI: 10.24425/mms.2022.143072

Table 9. Uncertainty calculation for diameter and depth measurements using DMI.

Source of uncertainty x_i	**Limit**	**Standard Uncertainty $u(x_i)$**	**Sensitivity coefficient c_i**	**Uncertainty $u(y_i)$ µm**
l_λ wavelength	2 nm	1 nm	1	0.001
l_{tm} (Δt_m steel)	0.1°	0.057 °	αL	$0.66L$
l_{tm} (Δt_m Al)	0.1°	0.057 °	αL	$1.37L$
l_α (α steel)	1×10^{-6}/°	0.57×10^{-6}/°	$tm\,L$	$0.28L$
l_α (α Al)	2.4×10^{-6}/°	1.39×10^{-6}/°	$tm\,L$	$0.69L$
l_{ta} Temp.	0.05°	0.025°	$9.6\times10^{-7}L$	$0.02L$
l_p Pressure	0.1 mmHg	0.057 mmHg	$0.3\times10^{-6}L$	$0.017L$
l_{RH} Humidity	3%	1.5%	$9.8\times10^{-9}L$	$0.01L$
l_S Res. Stage	0.5 µm	0.29 µm	1	0.29
l_r Res. Software	1 nm	0.57 nm	1	0.00057
Cosine error	0.5 µm	0.29 µm	1	0.29
l_g Geometry	—	50 nm	1	0.05
l_I Interferometer	1 nm	0.57 nm	1	0.00057
l_P Repeatability	—	0.6 µm	1	0.6

of the temperature of the blocks in the uncertainty budget is $0.66L$ and $1.37L$ for steel and aluminum blocks respectively in the case when the temperature reading is 20° and the resolution of the temperature sensor is 0.1°. The steel blocks had the thermal expansion of 11.5×10^{-6}/° with limits of 1×10^{-6}/° and that for aluminum is 24×10^{-6}/° with limits of 2.4×10^{-6}/° and their effect on uncertainty is about $0.2L$ and $0.69L$. The variation in the refractive index of the medium led to a change in the wavelength of the laser and so led to a change in the distance measured thus any deviation in the refractive index is compensated through the Edlén equation [20]. The errors in the Edlén equation due to the effect of temperature, humidity and pressure are 0.02 µm, 0.01 µm and 0.017 µm respectively. The repeatability of ten measurements contributes to uncertainty by 0.6 µm. In addition, the cosine error is one of the basic sources of uncertainty that comes from the misalignment between the laser beam and the axis of motion. The cosine error is determined according to [30]:

$$d_{\cos} = \frac{x^2}{8l}\,, \tag{10}$$

where x is the shift between the two reflected laser spots in mm and l is the length of motion in mm.

Finally, the combined uncertainty in the diameter and depth measurement process can be calculated through the equation:

$$u_c(l) = \sqrt{\begin{array}{l} u(l_\lambda)^2 + u(l_{tm})^2 + u(l_\alpha)^2 + u(l_{ta})^2 + u(l_p)^2 + u(l_{RH})^2 + \\ u(l_S)^2 + u(l_r)^2 + u(l_g)^2 + u(l_I)^2 + u(l_{\text{cosine}})^2 + u(l_P)^2 \end{array}} \tag{11}$$

The expanded uncertainty U_{95} with a coverage factor of 2 at a level of confidence of 95% is given as:

for steel block: $U_{95} = \pm 2\times\sqrt{0.53 + 0.51L^2}$,

for aluminum block: $U_{95} = \pm 2\times\sqrt{0.53 + 2.35L^2}$,

where L is the nominal length in meter.

4. Conclusions

As the industry progresses technologically, reference blocks have been produced by the authors in novel shapes to be utilized for ultrasonic calibration and non-destructive testing (NDT). The block properties such as micro-hardness, elastic moduli, and optical constants have been characterized. To ensure the accuracy of measurements, all results were acquired using conventional methods. The examination of blocks was carried out to establish the position, diameter, depth and angle of the FBHs. The results obtained using both ultrasonic and DMI approaches were mainly in agreement. They ensured that the new blocks could be used as reference blocks in a variety of applications. They can perform accurate FBH characterization, transducer sensitivity calibration, transducer dead zone calculation, and so forth. As a result, we conclude that the newly designed steel and aluminum blocks can be useful in calibration and NDT for a variety of industries, including petroleum pipes production, steel manufacturing and on the like. In the future we aim to complete the manufacturing of other reference blocks according to the industry requirements.

References

[1] Barakat, M. A. (2014). Ultrasonic inspection of composite resin restorative materials. *International Journal of Engineering & Technology IJET-IJENS, 14*(3), 1–5.

[2] Barakat, M. A. Y. (2018). Study of annealing influence on IrO2 thin films ultrasonic technique. *International Journal of Advanced Research (IJAR)*, *6*(9), 129–135. https://doi.org/10.21474/IJAR01/7653

[3] ASTM International. (2020). *Standard Practice for Fabrication and Control of Flat-Bottomed Hole Ultrasonic Standard Reference Blocks* (ASTM E127-20). https://doi.org/10.1520/E0127-20

[4] ASTM International. (2013). *Standard Practice for Fabrication and Control of Metal, Other than Aluminum, Reference Blocks Used in Ultrasonic Testing (Withdrawn 2019)* (ASTM E428-08).

[5] Blessing, G. V. (1983). Assessment of ultrasonic reference block calibration methodology. *Final Report National Bureau of Standards*.

[6] Zhang, Z., Yan, Y., Yu, X., Li, C., & Gong, L. (2022). A High-Precision and Wide Range Method for Inner Diameter Measurement. *Journal of Sensors*, 2022. https://doi.org/10.1155/2022/3985528

[7] Kazayawoko, M., Neumann, A. W., & Balatinecz, J. J. (1997). Estimating the wettability of wood by the Axisymmetric Drop Shape Analysis-contact Diameter method. *Wood Science and Technology*, *31*(2), 87–95. https://doi.org/10.1007/BF00705924

[8] Giulietti, N., Chiariotti, P., Cosoli, G., Mobili, A., Pandarese, G., Tittarelli, F., & Revel, G. M. (2021). Automated measurement system for detecting carbonation depth: Image-processing based technique applied to concrete sprayed with phenolphthalein. *Measurement*, *175*, 109142. https://doi.org/10.1016/j.measurement.2021.109142

[9] Falkner, A. H. (1978, December). Novel electro-optical instrument for profile measurement. *In Proceedings of the Institution of Electrical Engineers*, *125*(12), 1396–1399. IET Digital Library. https://doi.org/10.1049/piee.1978.0295

[10] Liangpanich, E., Akiyama, N., Yoshida, M., & Kuwabara, K. (2003). Analysis of measurement accuracy of quadrilateral hole using optical inner-diameter-measuring machine. *Optical Engineering*, *42*(9), 2568–2575. https://doi.org/10.1117/1.1598435

Metrol. Meas. Syst., Vol. 29 (2022), No. 4, pp. 719–736
DOI: 10.24425/mms.2022.143072

[11] Bahrawi, M., & Farid, N. (2010). Application of a commercially available displacement measuring interferometer to line scale measurement and uncertainty of measurement. *Mapan*, *25*(4), 259–264. https://doi.org/10.1007/s12647-010-0025-7

[12] Abdallah, A. W., Tutsch, R., & Nagib, N. N. (2018). Novel wide-angle ellipsometric arrangement for thin film thickness measurement. *Journal of Physics Communications*, *2*(5), 055007. https://doi.org/10.1088/2399-6528/aac084

[13] ASTM International. (1992). *Standard Practice for Fabrication and Control of Steel Reference Blocks Used in Ultrasonic Examination* (ASTM E428-05). https://doi.org/10.1520/E0428-05

[14] ASTM International. (2005). *Standard Practice for Fabrication and Control of Metal, Other than Aluminum Reference, Blocks Used in Ultrasonic Examination* (ASTM: E428-05a). https://doi.org/10.1520/E0428-08

[15] European Committee For Standardization. (2000). *Non-destructive testing – Characterization and verification of ultrasonic examination equipment – Part 3: Combined equipment* (BS EN 12668-3:2000). https://standards.iteh.ai/catalog/standards/cen/0e496e43-2c7f-40d6-8ade-625faf379068/en-12668-3-2000

[16] European Committee For Standardization. (2001), *Non-destructive testing. Characterization and verification of ultrasonic examination equipment. Probes* (BS EN 12668-2:2001). https://standards.iteh.ai/catalog/standards/cen/e2293225-8c90-481b-a689-0719f91c2307/en-12668-2-2010

[17] ASTM International. (2015). *Standard Practice for Measuring Thickness by Manual Ultrasonic Pulse-Echo Contact Method* (ASTM E797 / E797M-15). https://doi.org/10.1520/E0797_E0797M-21

[18] ASTM International. (2016). *Standard Practice for Evaluating Performance Characteristics of Ultrasonic Pulse-Echo Testing Instruments and Systems without the Use of Electronic Measurement Instruments*. https://doi.org/ASTM E317-16

[19] Haycocks, J., & Jackson, K. (2005). Traceable calibration of transfer standards for scanning probe microscopy. *Precision Engineering*, *29*(2), 168–175. https://doi.org/10.1016/j.precisioneng.2004.06.002

[20] Bönsch, G., & Potulski, E. (1998). Measurement of the refractive index of air and comparison with modified Edlén's formulae. *Metrologia*, *35*(2), 133. https://doi.org/10.1088/0026-1394/35/2/8

[21] Al-Shomar, S. M., Barakat, M. A., & Abdallah, A. W. (2020). Ellipsometric and ultrasonic studies of nano titanium dioxide specimens doped with Erbium. *Materials Research Express*, *7*(10), 106413. https://doi.org/10.1088/2053-1591/abc0d0

[22] Abdallah, A. W., & Abdelwahab, M. (2021). A modified method for calibration of polarimetric components using polarizing interferometry. *Measurement Science and Technology*, *32*(11), 115003. https://doi.org/10.1088/1361-6501/ac0fa7

[23] Abdallah, A. W., Abdelwahab, M., & El-Bahrawy, M. (2022). Developed Method to Evaluate Some Optical Parameters in Gauge Block Measurements Using Ellipsometry. *MAPAN*, 1–10. https://doi.org/10.1007/s12647-021-00521-6

[24] Barakat, M. A. Y. (2018). Amelioration of ultrasonic transducer to study CuO doped thin films. *Archives of Acoustics*, *43*(3), 487–495. https://doi.org/10.24425/123920

[25] Shehata, M., Abdallah, A. W., Ibrahim, S. S., Osman, M. H., & Nagib, N. N. (2021). Determination of a grown oxide layer thickness and optical constants of Zn and Cd metals. *Optik*, *232*, 166552. https://doi.org/10.1016/j.ijleo.2021.166552

[26] ASTM Standards. (1992). *Standard Practice for Fabricating and Checking Aluminum Alloy Ultrasonic Standard Reference Blocks* (E127-92a). https://doi.org/10.1520/E0127-98

[27] ASTM Standards. (1992). *Standard Practice for Measuring Ultrasonic Velocity in Materials* (ASTM-E494-92a – 1992A EDITION).

[28] Beers, J. S. (1987). Length scale measurement procedures at the National Bureau of Standards. *Interagency Report IR*, 87–3625.

[29] International Organization for Standardization (2008). *Uncertainty of measurement-Part 3: Guide to the expression of uncertainty in measurement* (GUM: 1995). https://www.iso.org/standard/50461.html

[30] Keysight Technologies. (1992). 5528A Laser Measurement System User Guide (User Manuals Part No. 05528-90022). https://www.keysight.com/ch/de/assets/9018-05832/user-manuals/9018-05832.pdf

[31] Palik, D. E. (Ed.). (1997). *Handbook of Optical Constants of Solids* (1st ed.). Academic Press. www.elsevier.com/books/handbook-of-optical-constants-of-solids/palik/978-0-08-055630-7

Associate Professor **Mirham A. Y. Barakat** works at the Department of Ultrasonic Metrology of the National Institute of Standards in Egypt. She has experience in ultrasonic calibration of many instruments such as flaw detectors, transducers, blocks and on the like. She conducted research on the amelioration of ultrasonic transducers, the study of cracks, the ultrasonic study of some materials, the manufacture of new piezoelectric materials and on the like. She also received awards from Cairo University, the National Institute of Standards and Hail University.

Mohamed Abdelwahab received the M.Sc. degree from the Department of Physics, Faculty of Science, Helwan University and the Ph.D. degree from the Al-Alzhar University. He works as a researcher at the Division of Length and Precision Engineering of the National Institute of Standards, Egypt. He has experience in optical and dimensional metrology, especially in interferometric measurement of gauge blocks and line scale, nonlinear optics and speckle metrology. His research concerns the displacement interferometer, speckle photography, gauge block measurements, absolute distance metrology, the calibration of the retardance using polarizing interferometry.

Alshaimaa Waheed Abdallah received her M.Sc. and Ph.D. degrees from the Department of Physics, Faculty of Science, Cairo University. She works as a researcher at the Division of Length and Precision Engineering of the National Institute of Standards, Egypt. She has experience in optical and dimensional metrology, especially in polarimetric and ellipsometric techniques, interferometric measurement of gauge blocks and line scale. Her research work concerns development of ellipsometric methods for material measurements, calibration of retardance using interferometry, gauge block measurements, measuring the optical and dimensional properties of materials with high accuracy.